Electronic Supplementary Material (ESI) for Physical Chemistry Chemical Physics.

Electronic Supplementary Information

Contents

1. Cartesian coordinates, UHCTH/407 energies, and $\langle S^2 \rangle$ values of **1**–**3** and **9**–**13**.

Cartesian coordinates of **1** optimized at the UHCTH/407/6-31G* level.

Center Number	Atomic Number	Atomic Type	Coordinates (Angstroms) X	Y	Z
1	7	0	0.000000	0.000000	-1.708049
2	6	0	0.000000	1.170228	-1.016218
3	6	0	0.000000	1.204506	0.412401
4	6	0	0.000000	0.000000	1.183266
5	6	0	0.000000	-1.204506	0.412401
6	6	0	0.000000	-1.170228	-1.016218
7	7	0	0.000000	2.307512	-1.728736
8	9	0	0.000000	2.369597	1.041293
9	7	0	0.000000	0.000000	2.508798
10	9	0	0.000000	-2.369597	1.041293
11	7	0	0.000000	-2.307512	-1.728736

E(UHCTH/407/6-31G*) = -608.749683960 Hartree

$\langle S^2 \rangle$ = 12.0854

Cartesian coordinates of **2** optimized at the UHCTH/407/6-31G* level.

Center Number	Atomic Number	Atomic Type	Coordinates (Angstroms) X	Y	Z
1	7	0	0.000000	0.000000	-1.946777
2	6	0	0.000000	1.169930	-1.259616
3	6	0	0.000000	1.220916	0.174854
4	6	0	0.000000	0.000000	0.931949
5	6	0	0.000000	-1.220916	0.174854
6	6	0	0.000000	-1.169930	-1.259616
7	7	0	0.000000	2.284817	-2.003643
8	17	0	0.000000	2.722360	0.979948
9	7	0	0.000000	0.000000	2.255095
10	17	0	0.000000	-2.722360	0.979948
11	7	0	0.000000	-2.284817	-2.003643

E(UHCTH/407/6-31G*) = -1329.63453431 Hartree

<S^2> = 12.0897

Cartesian coordinates of **3** optimized at the UHCTH/407/6-31G* level.

Center Number	Atomic Number	Atomic Type	Coordinates (Angstroms) X	Y	Z
1	7	0	0.000000	0.000000	2.259905
2	6	0	0.000000	1.169681	1.571121
3	6	0	0.000000	1.218211	0.139351
4	6	0	0.000000	0.000000	-0.616619
5	6	0	0.000000	-1.218211	0.139351
6	6	0	0.000000	-1.169681	1.571121
7	7	0	0.000000	2.285249	2.314979
8	35	0	0.000000	2.857269	-0.735239
9	7	0	0.000000	0.000000	-1.941184
10	35	0	0.000000	-2.857269	-0.735239
11	7	0	0.000000	-2.285249	2.314979

E(UHCTH/407/6-31G*) = -5555.31677723 Hartree

<S^2> = 12.0893

Cartesian coordinates of **9** optimized at the UHCTH/407/Sapporo-DZP-2012 level.

Center Number	Atomic Number	Atomic Type	Coordinates (Angstroms) X	Y	Z
1	6	0	0.000000	0.000000	-1.512480
2	6	0	0.000000	1.227556	-0.775103
3	6	0	0.000000	1.221988	0.605756
4	6	0	0.000000	0.000000	1.282667
5	6	0	0.000000	-1.221988	0.605756
6	6	0	0.000000	-1.227556	-0.775103
7	7	0	0.000000	0.000000	-2.840965
8	1	0	0.000000	2.165149	-1.330271
9	1	0	0.000000	2.148298	1.180062
10	9	0	0.000000	0.000000	2.622025

11	1	0	0.000000	-2.148298	1.180062
12	1	0	0.000000	-2.165149	-1.330271

E(UHCTH/407/Sapporo-DZP-2012) = -385.489491225 Hartree

$\langle S^2 \rangle$ = 2.0306

Cartesian coordinates of **10** optimized at the UHCTH/407/Sapporo-DZP-2012 level.

Center Number	Atomic Number	Atomic Type	Coordinates (Angstroms) X	Y	Z
1	6	0	0.000000	0.000000	-1.949167
2	6	0	0.000000	1.226362	-1.209103
3	6	0	0.000000	1.220171	0.170557
4	6	0	0.000000	0.000000	0.863579
5	6	0	0.000000	-1.220171	0.170557
6	6	0	0.000000	-1.226362	-1.209103
7	7	0	0.000000	0.000000	-3.274878
8	1	0	0.000000	2.165503	-1.761900
9	1	0	0.000000	2.156187	0.727741
10	17	0	0.000000	0.000000	2.586385
11	1	0	0.000000	-2.156187	0.727741
12	1	0	0.000000	-2.165503	-1.761900

E(UHCTH/407/Sapporo-DZP-2012) = -745.920465001 Hartree

$\langle S^2 \rangle$ = 2.0325

Cartesian coordinates of **11** optimized at the UHCTH/407/Sapporo-DZP-2012 level.

Center Number	Atomic Number	Atomic Type	Coordinates (Angstroms) X	Y	Z
1	6	0	0.000000	0.000000	-2.587747
2	6	0	0.000000	1.226304	-1.847999
3	6	0	0.000000	1.220649	-0.467567
4	6	0	0.000000	0.000000	0.222673
5	6	0	0.000000	-1.220649	-0.467567
6	6	0	0.000000	-1.226304	-1.847999
7	7	0	0.000000	0.000000	-3.913537

8	1	0	0.000000	2.165701	-2.400513
9	1	0	0.000000	2.159288	0.084822
10	35	0	0.000000	0.000000	2.114382
11	1	0	0.000000	-2.159288	0.084822
12	1	0	0.000000	-2.165701	-2.400513

E(UHCTH/407/Sapporo-DZP-2012) = -2861.22510531 Hartree

$\langle S^2 \rangle$ = 2.0326

Cartesian coordinates of **12** optimized at the UHCTH/407/Sapporo-DZP-2012 level.

Center Number	Atomic Number	Atomic Type	Coordinates (Angstroms) X	Y	Z
1	6	0	0.000000	0.000000	-3.086843
2	6	0	0.000000	1.225931	-2.346724
3	6	0	0.000000	1.220272	-0.966082
4	6	0	0.000000	0.000000	-0.271241
5	6	0	0.000000	-1.220272	-0.966082
6	6	0	0.000000	-1.225931	-2.346724
7	7	0	0.000000	0.000000	-4.412301
8	1	0	0.000000	2.165677	-2.898864
9	1	0	0.000000	2.163628	-0.421582
10	53	0	0.000000	0.000000	1.838286
11	1	0	0.000000	-2.163628	-0.421582
12	1	0	0.000000	-2.165677	-2.898864

E(UHCTH/407/Sapporo-DZP-2012) = -7210.23006717 Hartree

$\langle S^2 \rangle$ = 2.0329

Cartesian coordinates of **13** optimized at the UHCTH/407/DZVP level.

Center Number	Atomic Number	Atomic Type	Coordinates (Angstroms) X	Y	Z
1	7	0	0.000000	0.000000	2.493493
2	6	0	0.000000	1.169466	1.803340
3	6	0	0.000000	1.223196	0.371817
4	6	0	0.000000	0.000000	-0.377973

5	6	0	0.000000	-1.223196	0.371817
6	6	0	0.000000	-1.169466	1.803340
7	7	0	0.000000	2.283551	2.557405
8	53	0	0.000000	3.065450	-0.614548
9	7	0	0.000000	0.000000	-1.707148
10	53	0	0.000000	-3.065450	-0.614548
11	7	0	0.000000	-2.283551	2.557405

E(UHCTH/407/DZVP) = -14256.9130462 Hartree

$\langle S^2 \rangle$ = 12.0924

2. DFT calculations of the $\mathbf{D}^{SO}$ tensors of **1**–**3**.

The DFT-based $\mathbf{D}^{SO}$ tensor calculations of **1**–**3** were carried out using three following approaches: Pederson–Khanna (PK), coupled-perturbed (CP), and quasi-restricted orbital (QRO) approaches. We used six pure exchange–correlation functionals (LDA, BP86, BLYP, PBE, RevPBE, and TPSS) and three basis sets (Ahlrichs-DZ, cc-pVDZ, and cc-pVTZ). In **2** and **3**, the scalar relativistic calculations were carried out using the ZORA Hamiltonian,[1,2] in addition to the non-relativistic calculations. All the calculations were carried out at the UHCTH/407/6-31G* optimized geometry.

The theoretical D^{SO} values of **1**–**3** are summarized in Tables S1–S3, respectively. The D^{SO} values of **1**–**3** as calculated at the hybrid CASSCF/MRMP2 method are −0.0124 cm^{-1}, +0.0065 cm^{-1}, and −0.2537 cm^{-1}, respectively. As pointed out below, we emphasize that the DFT approaches here fail to reproduce our hybrid CASSCF/MRMP2 result.

In the DFT-based approaches, the direction of the D^{SO}_{ZZ} axis depends on both the theoretical methods and the basis sets. In **1,** all the DFT calculations except for QRO-TPSS give negative D^{SO} values, and the D^{SO}_{ZZ} axis is perpendicular to the molecular plane, which is consistent with our hybrid CASSCF/MRMP2 result. In **2**, the PK method gives the $\mathbf{D}^{SO}$ tensor in which the D^{SO}_{ZZ} axis is parallel to the direction connecting two chlorine atoms, and the other two methods (CP and QRO) predict the D^{SO}_{ZZ} axis to be perpendicular to the molecular plane. As discussed in the present study, the hybrid CASSCF/MRMP2 method predicts that the D^{SO}_{ZZ} axis is parallel to the C_2 symmetry axis, and therefore, importantly all the DFT approaches fail to reproduce our hybrid CASSCF/MRMP2 result even qualitatively. In **3**, the D^{SO}_{ZZ} axis is predicted to be parallel to the direction connecting two bromine atoms, in which case the PK or CO method is adopted in conjunction with the cc-pVDZ and cc-pVTZ basis sets. The QRO method and the CP method with Ahlrichs-DZ basis set give the D^{SO}_{ZZ} axis perpendicular to the molecular plane. In **3**, most calculations predict the positive sign of D^{SO}. Only the combination of the CP approach and Ahlrichs-DZ basis set gives negative D^{SO} values in **3**, but the magnitude of D^{SO} is too large to agree with the experiment, and the direction of the D^{SO}_{ZZ} axis is different from our hybrid CASSCF/MRMP2 result.

1 E. van Lenthe, E. J. Baerends and J. G. Snijders, *J. Chem. Phys.,* 1993, **99**, 4597–4610.

2 E. van Lenthe, J. G. Snijders and E. J. Baerends, *J. Chem. Phys.,* 1996, **105**, 6505–6516.

Table S1 Theoretical D^{SO} values of **1** as calculated by using the DFT approaches

		D^{SO}/cm^{-1}		
Functional	Basis set	PK	CP	QRO
LDA	Ahlrichs-DZ	−0.0089	−0.0129	−0.0040
	cc-pVDZ	−0.0085	−0.0122	−0.0041
	cc-pVTZ	−0.0101	−0.0145	−0.0046
BP86	Ahlrichs-DZ	−0.0069	−0.0105	−0.0013
	cc-pVDZ	−0.0066	−0.0100	−0.0015
	cc-pVTZ	−0.0076	−0.0116	−0.0012
BLYP	Ahlrichs-DZ	−0.0078	−0.0116	−0.0023
	cc-pVDZ	−0.0075	−0.0110	−0.0026
	cc-pVTZ	−0.0089	−0.0131	−0.0027
PBE	Ahlrichs-DZ	−0.0072	−0.0109	−0.0014
	cc-pVDZ	−0.0068	−0.0103	−0.0016
	cc-pVTZ	−0.0079	−0.0119	−0.0014
RevPBE	Ahlrichs-DZ	−0.0068	−0.0104	−0.0010
	cc-pVDZ	−0.0065	−0.0099	−0.0013
	cc-pVTZ	−0.0074	−0.0113	−0.0008
TPSS	Ahlrichs-DZ	−0.0056	−0.0089	+0.0003
	cc-pVDZ	−0.0053	−0.0084	−0.0005
	cc-pVTZ	−0.0060	−0.0097	+0.0004

Table S2 Theoretical D^{SO} values of **2** as calculated by using the DFT approaches. Values in parenthesis are the relativistic DFT results using ZORA Hamiltonian

		D^{SO}/cm^{-1}		
Functional	Basis set	PK	CP	QRO
LDA	Ahlrichs-DZ	+0.0171 (+0.0172)	−0.0621 (−0.0624)	+0.1898 (+0.1912)
	cc-pVDZ	+0.0142 (+0.0141)	−0.0498 (−0.0494)	+0.1480 (+0.1465)
	cc-pVTZ	+0.0164 (+0.0163)	−0.0608 (−0.0607)	+0.1889 (+0.1884)
BP86	Ahlrichs-DZ	+0.0125 (+0.0126)	−0.0529 (−0.0532)	+0.1689 (+0.1699)
	cc-pVDZ	+0.0105 (+0.0104)	−0.0433 (−0.0430)	+0.1385 (+0.1382)
	cc-pVTZ	+0.0117 (+0.0117)	−0.0523 (−0.0522)	+0.1754 (+0.1750)
BLYP	Ahlrichs-DZ	+0.0146 (+0.0147)	−0.0565 (−0.0567)	+0.1762 (+0.1774)
	cc-pVDZ	+0.0122 (+0.0121)	−0.0455 (−0.0452)	+0.1396 (+0.1382)
	cc-pVTZ	+0.0140 (+0.0140)	−0.0558 (−0.0557)	+0.1792 (+0.1788)
PBE	Ahlrichs-DZ	+0.0127 (+0.0129)	−0.0535 (−0.0538)	+0.1708 (+0.1720)
	cc-pVDZ	+0.0107 (+0.0106)	−0.0439 (−0.0435)	+0.1403 (+0.1389)
	cc-pVTZ	+0.0119 (+0.0119)	−0.0528 (−0.0527)	+0.1766 (+0.1763)
RevPBE	Ahlrichs-DZ	+0.0118 (+0.0118)	−0.0515 (−0.0518)	+0.1654 (+0.1665)
	cc-pVDZ	+0.0099 (+0.0098)	−0.0426 (−0.0423)	+0.1385 (+0.1372)
	cc-pVTZ	+0.0109 (+0.0109)	−0.0508 (−0.0507)	+0.1729 (+0.1726)
TPSS	Ahlrichs-DZ	+0.0094 (+0.0094)	−0.0457 (−0.0459)	+0.1457 (+0.1468)
	cc-pVDZ	+0.0079 (+0.0078)	−0.0386 (−0.0383)	+0.1278 (+0.1266)
	cc-pVTZ	+0.0087 (+0.0087)	−0.0464 (−0.0463)	+0.1602 (+0.1600)

Table S3 Theoretical D^{SO} values of **3** as calculated by using the DFT approaches. Values in parenthesis are the relativistic DFT results using ZORA Hamiltonian

		D^{SO}/cm^{-1}		
Functional	Basis set	PK	CP	QRO
LDA	Ahlrichs-DZ	+0.2911 (+0.3184)	−1.1922 (−1.3096)	+4.4348 (+4.8856)
	cc-pVDZ	+0.2545 (+0.2193)	+1.1960 (+1.0570)	+4.3017 (+3.8276)
	cc-pVTZ	+0.2884 (+0.2566)	+1.4471 (+1.3158)	+5.5162 (+5.0369)
BP86	Ahlrichs-DZ	+0.1962 (+0.2148)	−1.0247 (−1.1269)	+3.9214 (+4.3243)
	cc-pVDZ	+0.1713 (+0.1482)	+1.0289 (+0.9133)	+3.9856 (+3.5517)
	cc-pVTZ	+0.1871 (+0.1673)	+1.2374 (+1.1300)	+5.1055 (+4.6696)
BLYP	Ahlrichs-DZ	+0.2384 (+0.2610)	−1.0765 (−1.1826)	+4.0690 (+4.4811)
	cc-pVDZ	+0.2077 (+0.1794)	+1.0833 (+0.9593)	+4.0440 (+3.5991)
	cc-pVTZ	+0.2331 (+0.2080)	+1.3139 (+1.1978)	+5.2148 (+4.7681)
PBE	Ahlrichs-DZ	+0.1978 (+0.2166)	−1.0349 (−1.1390)	+3.9959 (+4.4096)
	cc-pVDZ	+0.1727 (+0.1494)	+1.0326 (+0.9166)	+4.0407 (+3.6008)
	cc-pVTZ	+0.1877 (+0.1681)	+1.2354 (+1.1291)	+5.1425 (+4.7063)
RevPBE	Ahlrichs-DZ	+0.1788 (+0.1959)	−1.0060 (−1.1081)	+3.9008 (+4.3073)
	cc-pVDZ	+0.1566 (+0.1357)	+1.0051 (+0.8936)	+3.9943 (+3.5623)
	cc-pVTZ	+0.1674 (+0.1502)	+1.1946 (+1.0933)	+5.0537 (+4.6299)
TPSS	Ahlrichs-DZ	+0.1372 (+0.1504)	−0.8882 (−0.9800)	+3.3625 (+3.7203)
	cc-pVDZ	+0.1208 (+0.1047)	+0.9241 (+0.8238)	+3.6809 (+3.2911)
	cc-pVTZ	+0.1293 (+0.1160)	+1.1105 (+1.0174)	+4.7038 (+4.3108)

3. UBP86/cc-pVDZ frontier orbitals of **3**.

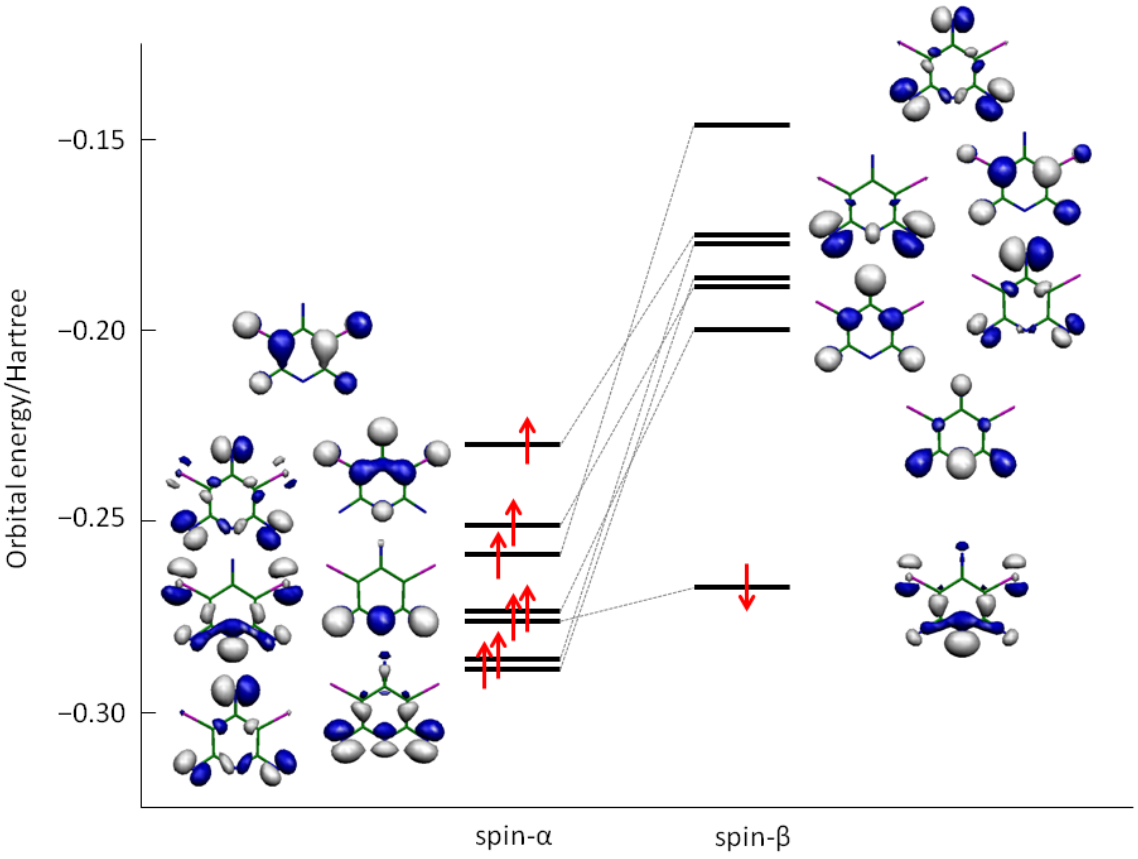

Fig. S1. UBP86/cc-pVDZ frontier orbitals of **3**. Red arrows denote electron occupations.

4. Spin configuration-based and orbital region partitioning-based analyses of the $\mathbf{D}^{SO}$ tensors of **1**, **2**, and **9**–**12** as calculated at PK-DFT.

The $\mathbf{D}^{SO}$ tensors calculated by means of Pederson–Khanna DFT approach can be analyzed in terms of the spin configuration-based method and the orbital region partitioning-based method, which has been proposed by us. All the calculations were carried out by using GAMESS-US software and laboratory-coded programs. The BP86 exchange–correlation functional was used for all the calculations. The cc-pVDZ and the Sapporo-DZP-2012 basis sets were used for **1** and **2**, and for **9**–**12**, respectively. The spin–orbit coupling integrals were evaluated using one-electron SOC Hamiltonian with effective nuclear charges (ZEFTYP=3-21G in GAMESS input). The decomposed $\mathbf{D}^{SO}$ tensors are given in Tables S4–S9.

Table S4 The decomposed $\mathbf{D}^{SO}$ tensor of **1** on the basis of the spin configurations and orbital region partitioning.

Excitations	D_{xx}/cm^{-1}	D_{yy}/cm^{-1}	D_{zz}/cm^{-1}
α → α	−0.03507	−0.03793	−0.03638
β → β	−0.03898	−0.04543	−0.04008
α → β	0.04251	0.06242	0.05716
β → α	0.03144	0.03202	0.02922
DOR → UOR	0.00002	0.00015	0.00010
SOR → UOR	−0.00003	−0.00006	−0.00005
DOR → SOR	0.00295	0.01130	0.00868
SOR → SOR	−0.00304	−0.00031	0.00118

Table S5 The decomposed $\mathbf{D}^{SO}$ tensor of **2** on the basis of the spin configurations and orbital region partitioning.

Excitations	D_{xx}/cm^{-1}	D_{yy}/cm^{-1}	D_{zz}/cm^{-1}
α → α	−0.73145	−0.63856	−0.69632
β → β	−0.73203	−0.71875	−0.73626
α → β	0.73596	0.75718	0.76823
β → α	0.72669	0.61812	0.67301
DOR → UOR	0.00065	0.00057	0.00078
SOR → UOR	−0.00071	−0.00092	−0.00138
DOR → SOR	0.00352	0.02267	0.00723
SOR → SOR	−0.00429	−0.00433	0.00203

Table S6 The decomposed $\mathbf{D}^{SO}$ tensor of **9** on the basis of the spin configurations and orbital region partitioning.

Excitations	D_{xx}/cm^{-1}	D_{yy}/cm^{-1}	D_{zz}/cm^{-1}
α → α	−2.23000	−2.75714	−1.16286
β → β	−2.07143	−2.52178	−1.10907
α → β	2.23702	2.76597	1.26205
β → α	2.06095	2.50999	1.07332
DOR → UOR	−0.00005	0.00027	0.00001
SOR → UOR	−0.00109	−0.00183	−0.00001
DOR → SOR	−0.00232	−0.00142	0.00836
SOR → SOR	0.00000	0.00000	0.05508

Table S7 The decomposed $\mathbf{D}^{SO}$ tensor of **10** on the basis of the spin configurations and orbital region partitioning.

Excitations	D_{xx}/cm^{-1}	D_{yy}/cm^{-1}	D_{zz}/cm^{-1}
α → α	−63.57499	−81.09573	−44.87691
β → β	−63.23203	−79.41198	−44.93132
α → β	63.41209	81.01547	45.15162
β → α	63.39056	79.47558	44.70543
DOR → UOR	0.00031	0.01017	0.00008
SOR → UOR	−0.00234	−0.02396	−0.00008
DOR → SOR	−0.00235	−0.00287	0.01048
SOR → SOR	0.00000	0.00000	0.03834

Table S8 The decomposed $\mathbf{D}^{SO}$ tensor of **11** on the basis of the spin configurations and orbital region partitioning.

Excitations	D_{xx}/cm^{-1}	D_{yy}/cm^{-1}	D_{zz}/cm^{-1}
α → α	−5988.45701	−6528.10178	−4464.22181
β → β	−5971.47814	−6406.47197	−4458.72340
α → β	5971.15302	6510.77034	4466.16947
β → α	5988.78324	6422.29560	4456.76789
DOR → UOR	0.11334	1.48831	0.00934
SOR → UOR	−0.10938	−2.96260	−0.01166
DOR → SOR	−0.00285	−0.03352	−0.00722
SOR → SOR	0.00000	0.00000	0.00170

Table S9 The decomposed $\mathbf{D}^{SO}$ tensor of **12** on the basis of the spin configurations and orbital region partitioning.

Excitations	D_{xx}/cm^{-1}	D_{yy}/cm^{-1}	D_{zz}/cm^{-1}
α → α	−30575.83214	−31869.52931	−24168.95133
β → β	−30536.72331	−31457.69619	−24161.25987
α → β	30532.77439	31853.89979	24200.00438
β → α	30579.79862	31470.03486	24129.99989
DOR → UOR	0.83321	3.99230	0.20160
SOR → UOR	−0.80813	−7.02860	−0.31688
DOR → SOR	−0.00753	−0.25456	−0.65933
SOR → SOR	0.00000	0.00000	0.56767